Life-Cycle of Structures and Infrastructure Systems – Biondini & Frangopol (Eds)

Seismic performance evaluation of masonry infilled RC frame retrofitted with BRBs

R. Chelapramkandy & J. Ghosh
Indian Institute of Technology Bombay, Mumbai, Maharashtra, India

F. Freddi
University College London, London, UK

ABSTRACT: Reinforced concrete (RC) frames with unreinforced masonry infill represents a widely used construction typology across the globe, including regions characterized by moderate to high seismicity. These structures have been often designed before the introduction of modern seismic design codes, are characterized by low ductility and high seismic vulnerability and are in need for seismic retrofitting to meet the current safety standards. However, it is important to highlight that, although considered as non-structural elements, masonry infills can significantly affect the seismic response of the structure. However, their role on the seismic performance of retrofitted RC structures has been generally neglected in literature. Among the different retrofitting strategies, the use of buckling-restrained braces (BRBs) represents an effective solution to improve the seismic performance of existing RC structures. This study investigates the interaction between the BRBs and masonry infill on seismic response of a case study frame.

1 INTRODUCTION

Reinforced concrete (RC) frames with unreinforced masonry infills represent a widely used construction typology for building structures worldwide, including regions characterized by moderate to high seismicity (Dolšek & Fajfar, 2008; Akan et al. 2022). Historical and recent earthquakes have demonstrated the high vulnerability of these structures, especially when designed before the introduction of modern seismic design codes (i.e. low ductile frames) (Rossetto & Elnashai, 2003; Freddi et al. 2017; Freddi et al. 2021a). This highlights the urgent need to identify efficient and effective retrofit solutions for such structures to meet the life safety and damage limitation requirements. Among others, the use of dissipative braces represents an efficient strategy to improve the seismic performance of such low ductile buildings (Freddi et al. 2013; Gutiérrez-Urzúa & Freddi, 2022). The introduction of these braces creates a dual load path for the seismic input and increases strength, stiffness, and ductility of existing frames (Freddi et al. 2021b). Therefore, when introduced within existing frames, these braces can protect structural and non-structural building components from damage by reducing their seismic demand. Among others, buckling-restrained braces (BRBs) represent a type of dissipative devices in which a sleeve provides buckling resistance to an unbonded core that resists the axial stress, hence allowing the BRB's core to develop axial yielding in compression in addition to that in tension ensuring an almost symmetric hysteretic behavior (Freddi et al. 2021c).

Due to their brittle nature, the strength and stiffness of the masonry infills are often disregarded during the design process. However, it has been demonstrated that, from one side, they can significantly affect the seismic response of the structures; on the other side, their damage represents a significant percentage of the economic losses. For these reasons, several approaches are proposed in literature for simulating the presence of masonry infills within the

DOI: 10.1201/9781003323020-502

frame. Among others, a common strategy is to idealize the masonry infills as single or multiple compressive equivalent struts characterized by a highly nonlinear behavior (Crisafulli et al. 2000; Dolšek & Fajfar, 2008).

The present paper investigates the potential interactions between the retrofit system based on BRBs and the masonry infills. The numerical results provide some insights into the ability of BRBs in protecting not only the RC frame from damage but also the masonry infills. The paper is organized as follows: Section 2 describes the methodology followed for the definition of seismic fragility curves for the infilled and retrofitted infilled case study frames considering different damage states. Section 3 presents the finite element modeling strategy for the frame, the masonry infills, and the BRB devices. Section 4 presents the definition of damage states thresholds (using pushover analysis), the assessment of the seismic demand (using nonlinear time-history analysis) and the definition of seismic fragility curves for the infilled and retrofitted infilled frames. Finally, Section 5 presents the conclusions along with some future research directions.

2 METHODOLOGY

A three-story, three-bay masonry-infilled RC frame designed for gravity loads alone is selected as the case study structure and modeled in OpenSees (McKenna et al. 2000). The structure is retrofitted with BRBs following the procedure outlined in Freddi et al. (2021c). Nonlinear static analyses are performed for both infilled and retrofitted infilled RC frames to determine the damage state (DS) threshold values in terms of global engineering demand parameter (*EDP*). The maximum interstory drift ratio (IDR_{max}) is assumed as global *EDP* to synthetically describe the response of the structure, and the DS threshold values are estimated by mapping IDR_{max} to local *EDPs,* such as material strain and cross-section strength. Cloud analyses are successively performed considering a ground motion set to evaluate the seismic performance of the structure and subsequently determine the samples of structural demand by accounting for the record-to-record variability. Probabilistic seismic demand models (PSDMs) are successively derived for the IDR_{max} using the average spectral acceleration (Sa_{avg}) as the intensity measure (*IM*) (Baker & Jayaram, 2008; Eads et al. 2015). This *IM* is selected as it allows accounting for the natural period elongation that is typically observed in infilled frames as a consequence of the damage experienced by the infills during the earthquake. Moreover, it allows comparing fragility curves of structures characterized by different natural periods (i.e. the infilled and retrofitted infilled RC frames in this case). The Sa_{avg} is defined as the spectral acceleration averaged over a period band, as given in Equation (1).

$$Sa_{avg}(T_1, T_2, \ldots T_n) = \left(\prod_{i=1}^{n} Sa(T_i)\right)^{1/n} \tag{1}$$

where, $Sa(T_i)$ is the spectral acceleration at i^{th} period, and T_1, T_2,... T_n are the '*n*' periods of interest. In the present study, this period band is assumed to span from the natural period of the stiffest structure (i.e. the retrofitted infilled RC frames) to the natural period of the more flexible structure (i.e. the bare frame).

PSDMs are established by using bilinear regression models (Tubaldi et al. 2016; Freddi et al. 2017; O'Reilly & Monteiro, 2019; Aljawhari et al. 2021) based on the following expression:

$$\ln(EDP) = [a_1 + b_1 \times \ln(IM)]H_1 + [a_2 + b_2 \times \ln(IM)](1 - H_1) + \ln(\varepsilon) \tag{2}$$

where, a_1, b_1, a_2, and b_2 are the regression coefficients, and H_1 is the step function with the value of $H_1 = 0$ when $IM > IM^*$ and value of $H_1 = 1$ when $IM \leq IM^*$, where IM^* is the intersection point of the two segments as shown in Figure 1. The value of the IM^* is obtained such that the fitted bilinear regressions maximize the goodness of fit coefficient (R^2) (Tubaldi et al. 2016).

Fragility curves are successively derived for the masonry-infilled RC frame with and without the BRBs. Fragility curves give the likelihood of meeting or exceeding a specific DS and

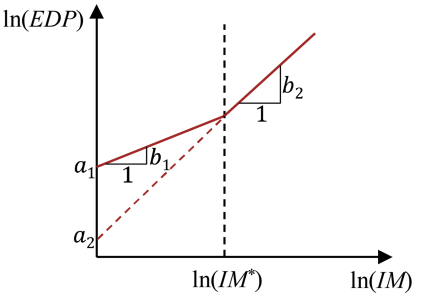

Figure 1. Bilinear probabilistic seismic demand model (PSDM) parameters.

are derived based on the PSDMs and DS threshold values according to the following expression:

$$P[DS|IM] = \Phi\left[\frac{\ln(EDP_{med}/S_C)}{\sqrt{\beta^2_{EDP|IM} + \beta^2_C}}\right] \tag{3}$$

where, EDP_{med} and $\beta_{EDP|IM}$ are the median estimates of seismic demand and corresponding standard deviation, whereas S_C and β_C are the DS threshold value and corresponding standard deviation.

3 CASE STUDY

3.1 *Case study description*

A three-story, three-bay RC frame representative of non-seismically designed (low ductility) low-rise building is selected for case study purposes. Figure 2 shows the elevation view of the frame, which has a bay width of 5.49 m and an interstory height of 3.66 m. The beams have a rectangular section of 230 mm × 460 mm, while the columns have a square section of 300 mm × 300 mm. The reinforcement bars have a yield strength of 276 MPa, whereas the concrete has a compressive cube strength of 24 MPa. Experimental results for the global and local response of the case study structure are available in literature (Aycardi et al. 1994; Bracci et al. 1995) and allowed the validation of the numerical model of the frame in OpenSees. Additionally, Figure 2 shows the considered unreinforced masonry infill with openings of 18% of the infill area, and the dissipative braces (i.e. D1 to D3).

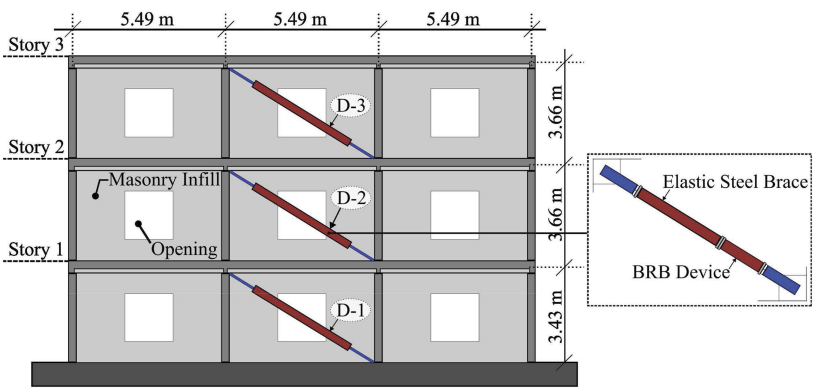

Figure 2. Case study infilled frame layout and placement of the dissipative braces.

3.2 *Finite element modeling of the RC frame*

The 2D model of the case study structure is developed in OpenSees. Columns and beams are modeled using the *beamWithHinges* element consisting of a central elastic part and two lateral portions with a specified length where a fiber approach is used to represent the nonlinear response of the section. The *Concrete02* and *Hysteretic* materials are used to model the concrete and longitudinal steel, respectively. The beam-to-column joints are modeled using four rigid offsets and a two-node *zeroLength* rotational springs. Additionally, shear and axial column failure are also modeled in OpenSees within *zeroLength* nonlinear springs. More details on the numerical model of the frame can be found in Freddi et al. (2013), (2017), (2021c).

3.3 *Finite element modeling of the masonry infills*

Unreinforced masonry infills within the RC frame are modeled following the recommendations of Dolšek & Fajfar (2008). The equivalent single diagonal strut modeling method is used to simulate the masonry infill behavior (Crisafulli et al. 2000; Wu et al. 2022). According to Dolšek & Fajfar (2008), the initial stiffness of the masonry infill can be defined as follows:

$$K_i = \frac{G_w L_{in} t_w}{H_{in}} \tag{4}$$

where, H_{in}, L_{in}, and t_w represents the height, length, and thickness respectively of the infill, and G_w is the infill shear modulus. The maximum force F_m of the masonry infill is determined as:

$$F_m = 0.818 \frac{L_{in} t_w f_{tp}}{C_I} \left(1 + \sqrt{{C_I}^2 + 1}\right), \text{ where, } C_I = 1.925 \frac{L_{in}}{H_{in}} \tag{5}$$

where, f_{tp} is the cracking strength of the masonry infill, and C_I is the coefficient that takes into account the interaction between the infills and the surrounding frame.

Figure 3 shows the force-displacement back-bone curve of the masonry infill - represented by four branches. The thickness of the infill is considered as 100 mm, and the shear strength and the shear modulus of the masonry infills are adopted from Hak et al. (2012) as 0.31 MPa and 1089 MPa, respectively. According to Dolšek & Fajfar (2008), the cracking force of the masonry infill (F_c) is assumed to be 60% of the maximum force (F_m). For the infill with the window, the story drift corresponding to the maximum force is considered 0.15%, whereas the story drift corresponding to the infill collapse is considered five times the story drift at the maximum force. The present paper considers a residual force (F_r) of 5% of the maximum force. Window opening covering one-third of the horizontal length of infill is considered as shown in Figure 2. The parameter λ_0 is used to reduce the infill's strength and initial stiffness in order to account for the masonry infill's opening, defined according to Equation (6) (Dolšek & Fajfar, 2008; Troup et al. 2019)

$$\lambda_0 = 1 - \frac{1.5 L_0}{L_{in}} \geq 0 \tag{6}$$

where, L_{in} and L_0 are, respectively, the total length of infill and horizontal length of openings.

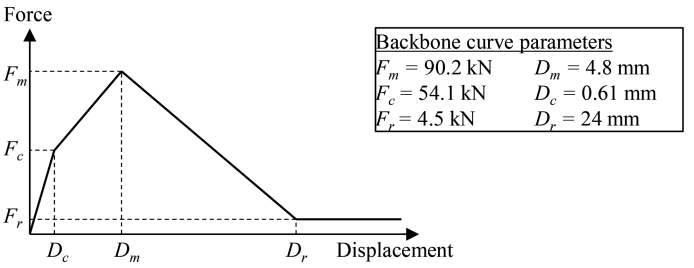

Figure 3. Lateral force-displacement envelope for the diagonal struts.

3.4 *Finite element modeling of the Buckling-Restrained Braces (BRBs)*

The design of the BRBs are based on the capacity curve of bare frame, and the retrofit design aims to double the retrofitted frame's base shear capacity (i.e. strength proportion coefficient $\alpha = 1$) (Freddi et al. (2021c)). The first mode shape of the retrofitted frame is maintained as same as that of the bare frame by properly proportioning the stiffness of BRBs in the frame, while the simultaneous yielding of the BRB device is ensured by properly proportioning the strength of BRBs among the stories. Each BRB consists of an elastic brace and a BRB device arranged in series. This study uses the *Steel02* material in OpenSees to model the BRB device. Additional details on the BRB design can be found in Freddi et al. (2021c). Table 1 lists the BRBs design properties where, $F_c^{\,i}$ and $K_c^{\,i}$ are the strength and stiffness, whereas $f_{y,BRB}$, L_{BRB}, and A_{BRB} are the yield strength, length, and area of cross-section of the BRB device core.

Table 1. Design properties of the BRBs and BRBs device core.

Story	$F_c^{\,i}$ (kN)	$K_c^{\,i}$ (kN/mm)	$f_{y,BRB}$ (MPa)	L_{BRB} (mm)	A_{BRB} (mm^2)
1	220.3	48.4	250	2815	881
2	189.6	32.6	250	3599	758
3	109.2	29.8	250	2270	437

4 SEISMIC FRAGILITY CURVES

4.1 *Threshold mapping of damage states*

Figure 4a shows the base shear vs. IDR_{max} results of the nonlinear static analyses performed for both the infilled and retrofitted infilled frames. The reduction in the base shear after attaining the peak value is related to the damage in the masonry infills. The DSs for the structural components are defined as Slight (S), Moderate (M), Extensive (E), and Complete (C) based on the distinct local responses of the structure listed in Table 2, along with the corresponding IDR_{max} at the onset of each DS. It is worthwhile to note that, due to the non-symmetric placement of the BRBs, nonlinear static analyses are carried out both in the positive and negative direction, providing slightly different capacity curves and DSs threshold values (marked in Figure 4a). Subsequently, the DS threshold values are taken as the average values from the two directions. For the infill panel, IDR_{max} value corresponding to the development of first crack on majority of infill at one floor is taken as threshold value corresponding to the Slight DS (SI). In order to incorporate the uncertainty in DS threshold estimation, a dispersion of 0.3 is assumed.

Table 2. Damage states description for infill panel, infilled frame and infilled frame retrofitted with BRBs.

	Description	Maximum IDR (%)	
Damage states	Building frame	Infilled	Infilled + BRBs
Slight	50% of columns at one floor have yielded	0.57	0.52
Moderate	50% of columns at one floor experienced concrete crushing	1.33	1.52
Extensive	Average of Moderate and Complete	2.16	2.32
Complete	50% of columns at one floor experienced shear failure initiation	3.00	3.12
	Infill panel		
Slight	Majority of infills at one floor develop first crack	0.019	0.019

4.2 *Probabilistic seismic demand model*

A set of 240 ground motion records from Baker et al. (2011) is used to perform the nonlinear time history analysis on the infilled frame and retrofitted infilled frame. The fundamental time period of the bare frame, infilled frame, and retrofitted infilled frame are 1.2s, 0.160s, and 0.156s, respectively. The period band considered for the calculation of the Sa_{avg} spans from 0.156s to 1.2s, with intervals of 0.1s. Figure 4b shows the bilinear PSDMs for both infilled frame and retrofitted infilled frame developed by following the approach discussed in Section 2. The results show a good fitting in both cases with R^2 values of 0.90 and 0.87. The expression of the bilinear PSDM, respectively, for the infilled and retrofitted infilled frames are as follows:

$$\ln[IDR_{\max}(\%)] = [-1.17 + 1.02 \times \ln(Sa_{avg})]H_1 + [1.11 + 2.37 \times \ln(Sa_{avg})](1 - H_1) \quad (7)$$

$$\ln[IDR_{\max}(\%)] = [-1.18 + 1.08 \times \ln(Sa_{avg})]H_1 + [0.46 + 2.50 \times \ln(Sa_{avg})](1 - H_1) \quad (8)$$

with values of IM^*, the intersection point of two segments, being equal to 0.18g and 0.32g for infilled and retrofitted infilled frames.

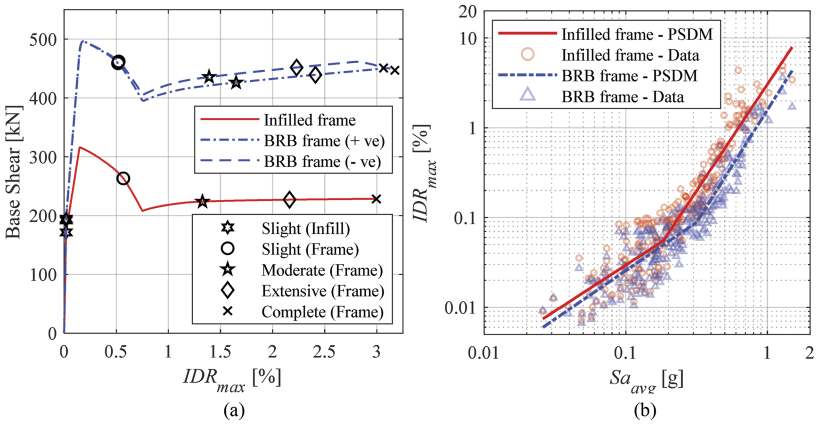

Figure 4. (a) Base shear vs. IDR_{max} curves and mapping of IDR_{max} values with different damage state thresholds; (b) Bilinear PSDMs of the infilled frame and retrofitted infilled frame.

4.3 *Seismic fragility curves*

Figure 5 shows the fragility curves for the infilled and retrofitted infilled frames. The median values of Sa_{avg} corresponding to different DSs are listed in Table 3. There is a significant decrease observed in the seismic fragility of the structural components after the retrofitting with BRBs, that is evident with the increases in the median values of Sa_{avg} for Slight, Moderate, Extensive, and Complete DS, respectively equal to 30%, 39%, 35%, and 32%. The advantages in protecting the infill panels from cracking is more modest. The comparison of the fragility curves shows an increase of 17% in the median values of Sa_{avg} for the Slight DS of the infill panels. This reduction in the seismic fragility shows the characteristics of the BRB device to provide a supplementary path to the lateral loads induced by the earthquake and to enhance the seismic performance by dissipating the earthquake energy. Moreover, a reduction in dispersion of 5.5% and 9.5% is observed, respectively, for the structural and non-structural components after the retrofitting with BRBs.

Table 3. Median values (in units of g) of lognormal fragility curves.

Structure type	Building frame				Infill panel
	Slight (S)	Moderate (M)	Extensive (E)	Complete (C)	Slight (SI)
Infilled frame	0.493	0.705	0.865	0.993	0.065
Infilled + BRB frame	0.641	0.984	1.166	1.312	0.076

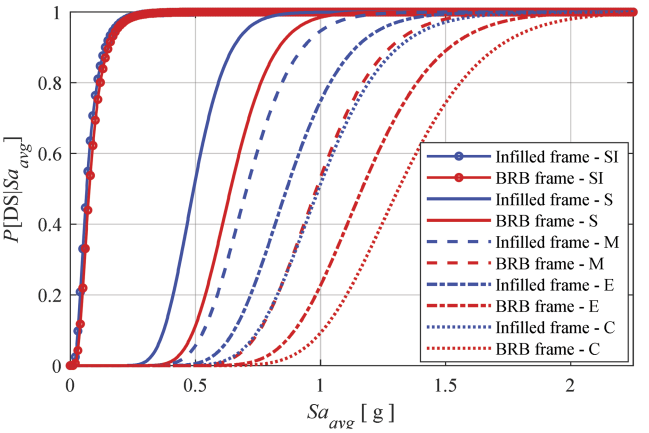

Figure 5. Seismic fragility curves of infilled and infilled frame retrofitted with BRBs.

5 CONCLUSIONS

The present study investigates the use of buckling-restrained braces (BRBs) for the seismic retrofitting of low ductility reinforced concrete (RC) frames. In particular the study focuses on the presence of masonry infills and their interaction with the BRBs. A three-story, three-bay masonry-infilled RC frame designed for gravity loads alone is selected as the case study structure and modeled in OpenSees. Masonry infills with openings are added to the model as single compressive diagonal struts in the two directions. Nonlinear static analyses were performed for both the infilled and retrofitted infilled frames for determining the DS thresholds, followed by the derivation of the PSDMs and fragility curves. The comparison of the fragility curves shows a significant improvement in the seismic performance of the structural components after the retrofitting with increases of the median Sa_{avg} values of 30%, 39%, 35%, and 32%, respectively for the Slight, Moderate, Extensive, and Complete DSs. A more modest increase (i.e. 17%) in the median value of Sa_{avg} was observed in the Slight DS of the infill panel. Future work may consider the different uncertainties for seismic evaluation of a retrofitted infilled frame and its life-cycle cost estimation.

REFERENCES

Akan O.D., O'Reilly G.J., & Monteiro R. 2022. Simplified modelling and pushover analysis of infilled frame structures accounting for strut flexibility. *Earthquake Engineering and Structural Dynamics* 51 (6): 1383–1409.

Aljawhari K., Gentile R., Freddi F., & Galasso C. 2021. Effects of ground-motion sequences on fragility and vulnerability of case-study reinforced concrete frames. *Bulletin of Earthquake Engineering* 19 (15): 6329–6359.

Aycardi L.E., Mander J.B., & Reinhorn A.M. 1994. Seismic resistance of reinforced concrete frame structures designed only for gravity loads: Experimental performance of subassemblages. *ACI Materials Journal* 91 (5): 552–563.

Baker J.W., & Jayaram N. 2008. Correlation of spectral acceleration values from NGA ground motion models. *Earthquake Spectra* 24 (1): 299–317.

Baker J.W., Lin T., Shahu S.K., & Jayaram N. 2011. New Ground Motion Selection Procedures and Selected Motions for the PEER Transportation Research Program. *Pacific Earthquake Engineering Research Center*.

Bracci J.M., Reinhorn A.M., & Mander J.B. 1995. Seismic resistance of reinforced concrete frame structures designed for gravity loads: performance of structural system. *ACI Materials Journal* 92 (5): 597–609.

Crisafulli F.J., Carr A.J., & Park R. 2000. Analytical modelling of infilled frame structures - A general review. *Bulletin of the New Zealand Society for Earthquake Engineering* 33 (1): 30–47.

Dolšek M., & Fajfar P. 2008. The effect of masonry infills on the seismic response of a four-storey reinforced concrete frame - a deterministic assessment. *Engineering Structures* 30 (7): 1991–2001.

Eads L., Miranda E., & G. Lignos Dimitrios. 2015. Average spectral acceleration as an intensity measure for collapse risk assessment. *Earthquake Engineering & Structural Dynamics* 44: 2057–2073.

Freddi F., Ghosh J., Kotoky N., & Raghunandan M. 2021c. Device uncertainty propagation in low-ductility RC frames retrofitted with BRBs for seismic risk mitigation. *Earthquake Engineering and Structural Dynamics* 50 (9): 2488–2509.

Freddi F., Novelli V., Gentile R., Veliu E., Andreev S., Andonov A., Greco F., & Zhuleku E. 2021a. Observations from the 26th November 2019 Albania earthquake: the earthquake engineering field investigation team (EEFIT) mission. *Bulletin of Earthquake Engineering* 19 (5): 2013–2044.

Freddi F., Padgett J.E., & Dall'Asta A. 2017. Probabilistic seismic demand modeling of local level response parameters of an RC frame. *Bulletin of Earthquake Engineering* 15 (1): 1–23.

Freddi F., Tubaldi E., Ragni L., & Dall'Asta A. 2013. Probabilistic performance assessment of low-ductility reinforced concrete frames retrofitted with dissipative braces. *Earthquake Engineering & Structural Dynamics* 42: 993–1011.

Freddi F., Tubaldi E., Zona A., & Dall'Asta A. 2021b. Seismic performance of dual systems coupling moment resisting and buckling-restrained braced frames. *Earthquake Engineering & Structural Dynamics* 50: 329–353.

Gutiérrez-Urzúa F., & Freddi F. 2022. Influence of the design objectives on the seismic performance of steel moment resisting frames retrofitted with buckling restrained braces. *Earthquake Engineering & Structural Dynamics* 51: 3131–3153.

Hak S., Morandi P., Magenes G., & Sullivan T.J. 2012. Damage control for clay masonry infills in the design of RC frame structures. *Journal of Earthquake Engineering* 16 (SUPPL. 1): 1–35.

McKenna F., Fenves G.L., & Scott M.H. 2000. Open System for Earthquake Engineering Simulation. *Pacific Earthquake Engineering Research Center*

O'Reilly G.J., & Monteiro R. 2019. Probabilistic models for structures with bilinear demand-intensity relationships. *Earthquake Engineering and Structural Dynamics* 48 (2): 253–268.

Rossetto T., & Elnashai A. 2003. Derivation of vulnerability functions for European-type RC structures based on observational data. *Engineering Structures* 25 (10): 1241–1263.

Troup L., Phillips R., Eckelman M.J., & Fannon D. 2019. Effect of window-to-wall ratio on measured energy consumption in US office buildings. *Energy and Buildings* 203: 109434.

Tubaldi E., Freddi F., & Barbato M. 2016. Probabilistic seismic demand model for pounding risk assessment. *Earthquake Engineering & Structural Dynamics* 45: 1743–1758.

Wu J.R., Di Sarno L., Freddi F., & D'Aniello M. 2022. Modelling of masonry infills in existing steel moment-resisting frames: Nonlinear force-displacement relationship. *Engineering Structures* 267.